

Dilution of Disposal Orbit Collision Risk for the Medium Earth Orbit Constellations

13 May 2005

Prepared by

A. B. JENKIN
Astrodynamics Department
Systems Engineering Division

and

R. A. GICK
Performance Modeling and Analysis Department
System Performance and Exploitation

Prepared for

SPACE AND MISSILE SYSTEMS CENTER
AIR FORCE MATERIEL COMMAND
2430 E. El Segundo Boulevard
Los Angeles Air Force Base, CA 90245

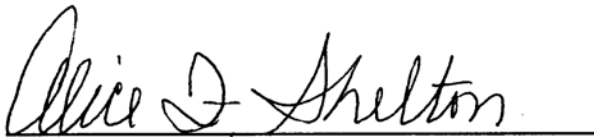
Engineering and Technology Group

APPROVED FOR PUBLIC RELEASE;
DISTRIBUTION UNLIMITED

This report was submitted by The Aerospace Corporation, El Segundo, CA 90245-4691, under Contract No. FA8802-04-C-0001 with the Space and Missile Systems Center, P.O. Box 92960, Los Angeles AFB, CA 90009-2960. It was reviewed and approved for The Aerospace Corporation by Dr. David R. Hickman, General Manager, Systems Engineering Division. Alice F. Shelton was the project officer.

This report has been reviewed by the Public Affairs Office (PAS) and is releasable to the National Technical Information Service (NTIS). At NTIS, it will be available to the general public, including foreign nationals.

This technical report has been reviewed and is approved for publication. Publication of this report does not constitute Air Force approval of the report's findings or conclusions. It is published only for the exchange and stimulation of ideas.

A handwritten signature in cursive script, reading "Alice F. Shelton", written over a horizontal line.

Alice F. Shelton, SMC/AXFV
Project Officer

REPORT DOCUMENTATION PAGE				Form Approved OMB No. 0704-0188	
<p>The public reporting burden for this collection of information is estimated to average 1 hour per response, including the time for reviewing instructions, searching existing data sources, gathering and maintaining the data needed, and completing and reviewing the collection of information. Send comments regarding this burden estimate or any other aspect of this collection of information, including suggestions for reducing the burden, to the Department of Defense, Executive Services and Communications Directorate (0704-0188). Respondents should be aware that notwithstanding any other provision of law, no person shall be subject to any penalty for failing to comply with a collection of information if it does not display a currently valid OMB control number.</p> <p>PLEASE DO NOT RETURN YOUR FORM TO THE ABOVE ORGANIZATION.</p>					
1. REPORT DATE (DD-MM-YYYY) 30 September 2005		2. REPORT TYPE Technical Report		3. DATES COVERED (From - To)	
4. TITLE AND SUBTITLE Dilution of Disposal Orbit Constellation Risk for the Medium Earth Orbit Constellations				5a. CONTRACT NUMBER FA8802-04-C-0001	
				5b. GRANT NUMBER	
				5c. PROGRAM ELEMENT NUMBER	
6. AUTHOR(S) Alan B. Jenkin and R. Anne Gick				5d. PROJECT NUMBER	
				5e. TASK NUMBER 850600	
				5f. WORK UNIT NUMBER	
7. PERFORMING ORGANIZATION NAME(S) AND ADDRESS(ES) The Aerospace Corporation P. O. Box 92957 Los Angeles, CA 90009-2957				8. PERFORMING ORGANIZATION REPORT NUMBER TR-2005(8506)-2	
9. SPONSORING/MONITORING AGENCY NAME(S) AND ADDRESS(ES) USAF Space and Missile Systems Center Air Force Space Command 2430 E. El Segundo Blvd. Los Angeles Air Force Base, CA 90245				10. SPONSOR/MONITOR'S ACRONYM(S) SMC/AXFV	
				11. SPONSOR/MONITOR'S REPORT NUMBER(S) SMC-TR-05-19	
12. DISTRIBUTION/AVAILABILITY STATEMENT Approved for public release; distribution unlimited					
13. SUPPLEMENTARY NOTES					
14. ABSTRACT <p>Previous studies have shown that disposal orbits for the medium Earth orbit constellations can be unstable and undergo significant long-term eccentricity growth. This can lead to repenetration of the constellations by disposed vehicles, thereby posing a collision risk. The study presented here investigated the possibility of diluting disposal orbit collision risk by exploiting long-term eccentricity growth. The Galileo constellation was selected as an example. Various disposal strategies were considered. It was found that high eccentricity growth strategies can reduce the combined constellation and intra-graveyard collision risk relative to a minimum eccentricity growth strategy. High eccentricity growth strategies also offer the option of significantly increasing the percentage of disposed vehicles that will re-enter the atmosphere within 200 years after disposal rather than remain on orbit for thousands of years. High eccentricity growth strategies thereby offer an effective and potentially inexpensive option for medium Earth orbit debris mitigation.</p>					
15. SUBJECT TERMS Powerpoint presentations					
16. SECURITY CLASSIFICATION OF:			17. LIMITATION OF ABSTRACT	18. NUMBER OF PAGES 37	19a. NAME OF RESPONSIBLE PERSON Alan B. Jenkin
a. REPORT UNCL	b. ABSTRACT UNCL	c. THIS PAGE UNCL			19b. TELEPHONE NUMBER (Include area code) 310.336.2661

Acknowledgments

This work reflects research conducted under U.S. Air Force Space and Missile Systems Center Contract FA8802-04-C-0001. The authors wish to thank several individuals for their support of this work and assistance in preparing this paper. Technical committee members W. S. Campbell, C.C. Chao, and S.L. Hast provided technical review of the paper. W. S. Campbell commissioned the study and provided internal programmatic support for this work. A.F. Shelton, SMC/AXFV, provided external programmatic review and funding support. D.J. Dulaney provided publication review.

Table of Contents

1.	Introduction.....	1
2.	Overall Methodology.....	3
3.	Long-Term Orbit Propagation	5
4.	Collision Risk Analysis.....	7
5.	Constellation Model.....	9
6.	Concept Of Collision Risk Dilution.....	13
7.	Disposal Orbit Evolution For $E_0 = 0.005$	15
8.	The Minimum Eccentricity Growth Strategy.....	19
9.	High Eccentricity Growth Strategies	23
10.	Conclusions.....	31
	References.....	33

1. Introduction

The potential instability of disposal orbits of the Global Positioning System (GPS) was discovered by Chao (2000). The instability manifests itself as significant growth in orbital eccentricity over a timeframe of decades. The cause of this long-term eccentricity growth is a dynamical resonance condition resulting from the combined gravitational pull of the Sun, Moon, and the non-spherical gravity field of the Earth. Long-term eccentricity growth of disposal orbits will lead to penetration of the constellation by previously disposed vehicles, thereby posing a collision risk to the operational constellation members.

Chao and Gick (2002) also showed that disposal orbits for Glonass and Galileo can be similarly unstable. Hence, long-term disposal orbit eccentricity growth affects all of the existing and planned satellite constellations in medium Earth orbit (MEO).

Gick and Chao (2001) showed that the amount of eccentricity growth depends on the initial elements of the disposal orbit. In particular, minimization of the disposal orbit initial eccentricity, e_0 , and proper selection of the initial argument of perigee, ω_0 , can suppress eccentricity growth, and hence constellation penetration, over a time period of up to 200 years. The initial right ascension of ascending node ($RAAN = \Omega_0$) and inclination, i_0 , also strongly influence long-term eccentricity growth (Chao and Gick, 2002), but these orbital parameters are not easily modified during the disposal process due to the excessive amount of required ΔV .

Jenkin and Gick (2001, 2002) determined the long-term collision risk posed to the operational GPS constellation by disposed vehicles placed in orbits with perigees 500 km and 832 km above semi-synchronous orbit. In these cases, the disposal strategy that was modeled involved achieving a low initial eccentricity of 0.005. The initial argument of perigee was not selected to minimize eccentricity growth, but instead to yield average eccentricity growth after 200 years. The intent was to model the average collision risk that would result if ω_0 were allowed to take on random values.

Jenkin and Gick (2003) also determined the long-term collision risk posed to the operational GPS constellation by disposed upper stages that cannot raise their disposal orbit perigees outside of the constellation. The disposal orbits of these upper stages have relatively high apogees above the constellation, and therefore significant initial eccentricity. As a result, the upper stage disposal orbits undergo more rapid eccentricity growth than would occur if the vehicles were disposed with perigee 500 km above the constellation, with low e_0 and random ω_0 . The study showed that the early collision risk posed to the constellation by the upper stage disposal orbits with perigee left in the constellation will be higher than if the vehicles were disposed with perigee 500 km above the constellation (with low e_0 and random ω_0). However, eventually the collision risk posed by the case of vehicle disposal at 500 km would catch up and exceed the collision risk posed by the upper stage disposal orbits. It was evident that the faster eccentricity growth of the upper stage disposal orbits results in a dilution of the long-term collision risk.

The purpose of the study presented here is to investigate the possibility of diluting MEO disposal orbit collision risk by selection of e_0 and ω_0 in order to control long-term eccentricity growth. The Galileo constellation was selected as an example.

2. Overall Methodology

The study analysis flow was as follows. The long-term evolution of the expected range of constellation orbits was simulated using a mean element propagator of high accuracy to account for eccentricity growth. From the resulting data, a statistical spatial distribution model of the operational constellation was generated. Next, for each disposal strategy considered, the entire expected range of disposal orbit initial conditions was swept out, and the resulting disposal orbits were propagated over 200 years. The propagated disposal orbit histories and the constellation spatial density model were then used to generate an ensemble of time profiles of cumulative long-term collision probability, one for each disposal orbit initial condition. The total collision risk accounting for on-going disposal of satellites over time was determined by randomly selecting collision probability time profiles from the ensemble that was generated, time-shifting them to account for future disposal epochs, and then summing them together. The entire disposal sequence over 200 years is repeated 1000 times in Monte Carlo fashion. The overall methodology is depicted in Figure 1.

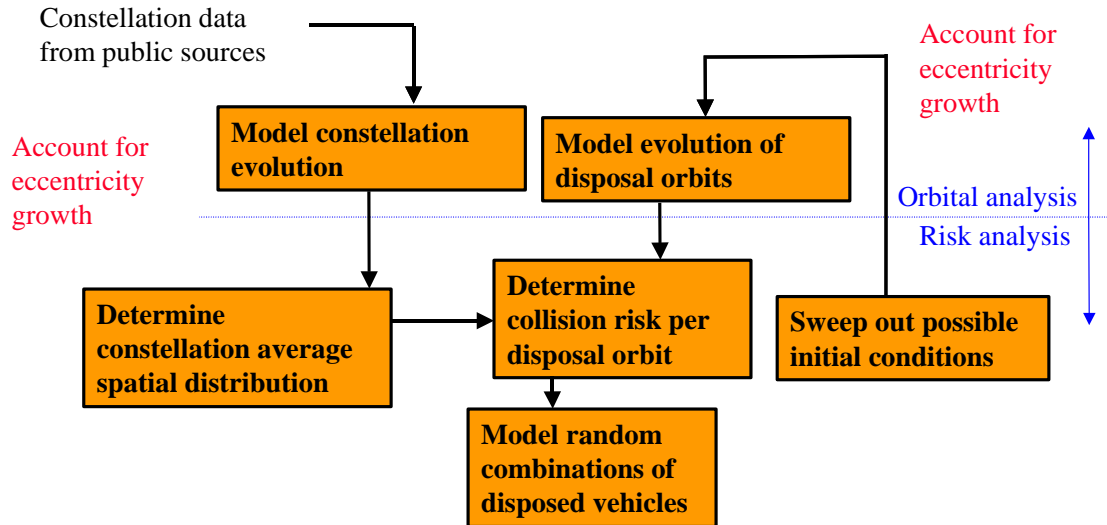


Figure 1. Overall study methodology.

3. Long-Term Orbit Propagation

The Aerospace Corporation tool MEANPROP was used to perform the long-term propagation of the constellation and disposal orbits. MEANPROP is a mean orbit element control simulation that uses the Semi-Analytic Orbit Propagator (SAOP) to perform long-term propagation. SAOP is a program developed by the Charles Stark Draper Laboratory that has undergone extensive validation (McLain, 1977). In this study, the force model included Sun-Moon gravity, a 12×12 WGS84 Earth gravity field, solar radiation pressure, and atmospheric drag. For modeling the effect of solar radiation pressure, vehicle design data on the GSTB-V2-B experimental Galileo satellite was taken from Space Daily (2004). As a result, the vehicle mass was assumed to be 523 kg, projected average cross-sectional area was assumed to be 4.53 m^2 (obtained by prorating GPS area by the Galileo power level), and the reflectivity coefficient c_r was assumed to be 1.3. For modeling the effect of atmospheric drag, the MSIS-90 atmosphere model was used, the solar flux parameter F10.7 was set to a constant value of 140, the geomagnetic index A_p was set to a constant value of 10, and the drag coefficient was assumed to be 2.0.

4. Collision Risk Analysis

A density-based method was used to compute collision risk in this study. This method is formulated from the perspective of the primary satellite as it flies through a field of secondary objects. The following formulation was used:

$$N_C(t) = A_{cc} \int_{t_0}^t \rho(r_s(\tau)) v d\tau \quad (1)$$

$$p_C(t) = 1 - e^{-N_C(t)} \quad (2)$$

where t is the current time point, t_0 is the propagation start epoch, $p_C(t)$ is the cumulative collision probability at time t , $N_C(t)$ is the average number of collisions at time t , r_s is the position of the primary satellite, $\rho(r_s)$ is spatial density (averaged over latitude and time) of the secondary objects at the position of the primary satellite, v is the average relative velocity between the primary and secondary satellites, and A_{cc} is the average collision cross-sectional area between the primary and secondary satellites.

The average collision cross-sectional area A_{cc} was set to unity, thereby normalizing the collision probability. This was done because little information was available in the open literature on the Galileo spacecraft design. Since the focus of this study is a comparison of the effectiveness of different disposal strategies on collision probability, the absolute level of the collision probability is not necessary. It is sufficient to compare collision probabilities normalized by cross-sectional area. It is a simple matter to obtain the absolute collision probability level by scaling the normalized probabilities with actual collision cross-sections determined from design information.

In order to accelerate computer processing, the integration in Eq. 1 was implemented using the method of averaging. This involves separating the problem into a short time-scale problem and a long time-scale problem. The short time-scale problem consists of determining the average number of collisions over a single orbit revolution of the primary satellite for an instance of mean orbital elements that have been propagated to a given epoch by MEANPROP. The average number of collisions per revolution is then divided by the orbit period to yield the average rate of growth of average number of collisions at the given mean orbital element epoch.

$$\left\langle \frac{dN_C}{dt} \right\rangle(t_L) = \frac{1}{T_p} A_{cc} \int_0^{T_p} \rho(r_s(\tau_s)) v d\tau_s \quad (3)$$

where T_p is the orbital period of the primary satellite. The long time-scale problem then consists of integrating Eq. 3.

$$N_C(t_L) = \int_{t_0}^t \left\langle \frac{dN_C}{d\tau} \right\rangle(\tau_L) d\tau_L \quad (4)$$

A computer program was used that evaluates Eq. 3 at each time point in the mean orbit element histories (i.e., at each long time-scale point). It then evaluates the integral in Eq. 4 (and subsequently Eq. 2) via a discrete trapezoidal algorithm that processes the results of Eq. 3 at those time points. This program was used to generate profiles of cumulative collision probability vs. time for each instance of initial disposal orbit conditions.

The density-based method used in this study was selected because it is computationally fast. However, it is an approximate technique that is less accurate than the miss distance-based method that has been used by the authors (Jenkin and Gick, 2001, 2002). It does not account for the correlations that exist between the disposal orbit and the constellation satellite orbits. In particular, there are correlations between the two orbit classes in Ω and ω because they evolve slowly, especially relative to each other. However, the values of Ω for the constellation planes are uniformly spaced as a whole (albeit deterministically and not randomly), and the initial values of ω of the constellation slots are randomly distributed throughout the constellation. As a result, the accuracy loss of the density-based method is not severe.

To demonstrate this fact, a numerical comparison between the two methods was performed for a GPS disposal case taken from Jenkin and Gick (2002). In this case, six vehicles are disposed at 500 km, one in each constellation plane. These vehicles subsequently penetrate the GPS constellation due to orbital eccentricity growth. Using each method, the collision probability time profiles over 200 years were computed and then averaged together into a single profile. The averaged profiles resulting from the two methods are presented in Fig. 2. This plot shows that, for the case considered, the density-based method generated a collision probability profile that is higher than that computed by the miss distance-based method by a factor of at most 1.4. Given other uncertainties in the problem (constellation configuration, satellite replacement rates, disposal orbit initial conditions, collision radii), this deviation is considered to be acceptable for this study.

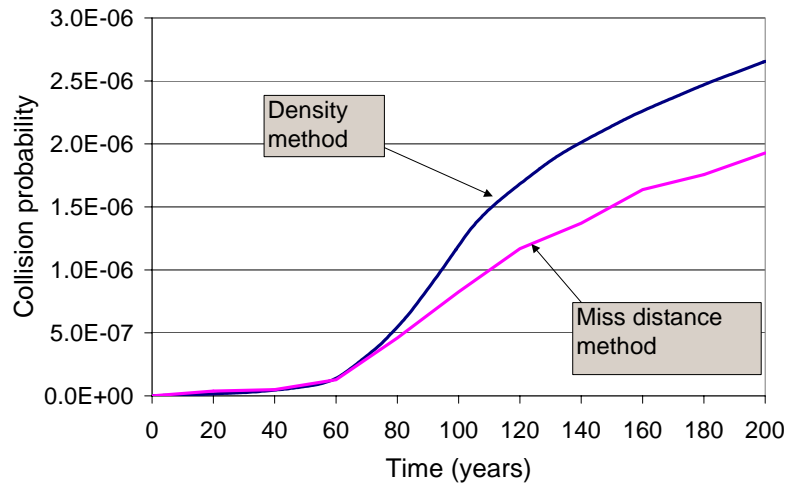


Figure 2. Comparison of methods for computing collision risk. Results are for a GPS disposal case taken from Jenkin and Gick (2002).

5. Constellation Model

In order to account for the effect of eccentricity growth on the orbital configuration of the constellation, the mean elements of constellation orbits were propagated over an assumed lifespan of the satellites. It was assumed that satellite station keeping maneuvers are carried out in a way so that they do not directly change eccentricity. This assumption is taken from the practice for GPS (Jenkin and Gick, 2001). The effect of station keeping on in-track position was not modeled. Therefore, the longitude of ascending node was allowed to drift in the propagation runs. It is not necessary to model the effect of station keeping on the in-track position because the in-track position has no effect on long-term collision probability. The formulation of collision probability used in this study (described below) is based on the assumption that the in-track position (i.e., argument of latitude) of the disposed vehicle relative to the satellite is continually randomized over 360 deg. This assumption is valid due to the difference between the semimajor axes of the disposed vehicle and the constellation satellites. This difference in semimajor axes causes a large enough difference in orbital mean motions to produce continual re-circulation of the disposed vehicle relative to the satellite over 360 deg with a repeat period of days to weeks (depending on the disposal orbit semimajor axis).

The propagation start epoch is assumed to be 1 January 2009. The initial semimajor axis of constellation orbits was assumed to be 29994 km, and inclination was assumed to be 56 deg (ESA, 2002). The orbital eccentricity was assumed to have an initial value of 0.008, which is taken from GPS practice (Jenkin and Gick, 2002).

The constellation orbits will undergo nodal regression due to the J_2 oblateness term of the Earth's gravitational field. The nodal regression rate for the Galileo constellation is 9.025 deg/year. Together, all three constellation planes will sweep out the entire 360 deg range of right ascension of ascending node, Ω , in 13.3 years. In addition, the argument of perigee, ω , may take on any value over its 360 deg range. Therefore, to generate the constellation model, the initial values Ω_0 and ω_0 were varied over the range $[0,360)$ deg in 10 deg increments. (The notation $[0,360)$ deg denotes the entire range from 0 deg to 360 deg, including 0 deg but excluding 360 deg because it is redundant with 0 deg.) Orbital mean element vs. time profiles for each (Ω_0, ω_0) pair were generated by propagating over a time period of 15 years using MEANPROP. This time period is based on the assumption that the maximum vehicle life is 15 years.

Figure 3 shows the resulting evolution of apogee and perigee altitude (relative to the constellation reference orbit) for a sample set of constellation orbits with $\Omega_0 = 180$ deg. Each curve corresponds to a specific value of ω_0 .

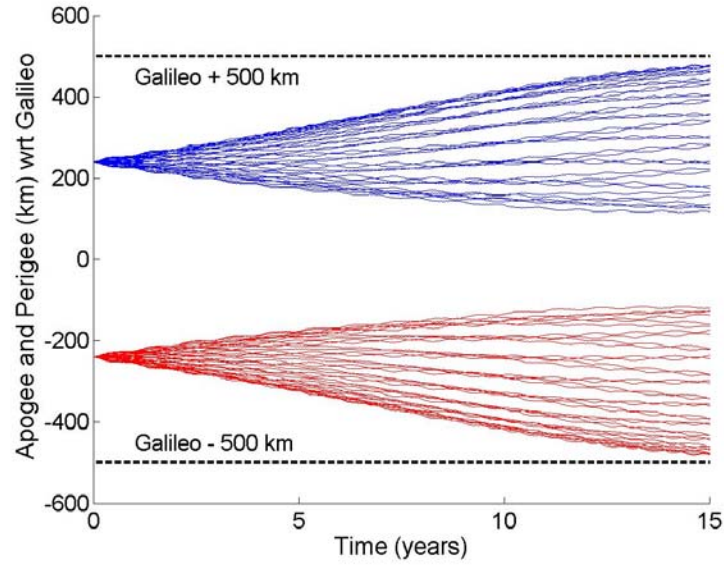


Figure 3. Apogee and perigee altitude profiles of Galileo constellation orbits (shown relative to the constellation reference orbit). Curves are shown for $\Omega_0 = 180$ deg and values of ω_0 that span the range $[0, 360)$ deg in 10 deg increments.

A statistical model of the spatial distribution of the constellation satellites was generated to support the collision risk analysis in this study. More specifically, the spatial number density as a function of altitude was computed. This distribution was determined as follows. The spatial density distribution over altitude at each time point in the MEANPROP long-term propagation files was computed using the formulation of satellite altitude distribution derived by Dennis (1972). This formulation is equivalent to the one derived by Kessler (1981). The resulting spatial density distributions for each time point are intrinsically averaged over latitude. These spatial density distributions were then averaged across all the propagation time points and (Ω_0, ω_0) pairs, and then prorated by the number of constellation members, which is assumed to be 30 (ESA, 2002). The resulting constellation spatial density distribution assumes that the Ω and ω for the orbits are randomly and uniformly distributed over 360 deg. This model therefore is a statistically stationary (i.e., static) representation of the constellation that accounts for replacement of satellites in a random order at an average rate of 2 satellites per year ($= 30$ constellation satellites \div 15 year satellite life).

Figure 4 shows the resulting average spatial density distribution. It can be seen from this figure that altitude boundaries at ± 500 km (relative to the constellation reference orbit) effectively clear the Galileo constellation most of the time. A disposal keepout zone of ± 500 km is a useful reference because it is the keepout zone that is specified for the semi-synchronous orbit by the U.S. Government Debris Mitigation Standard Practice.

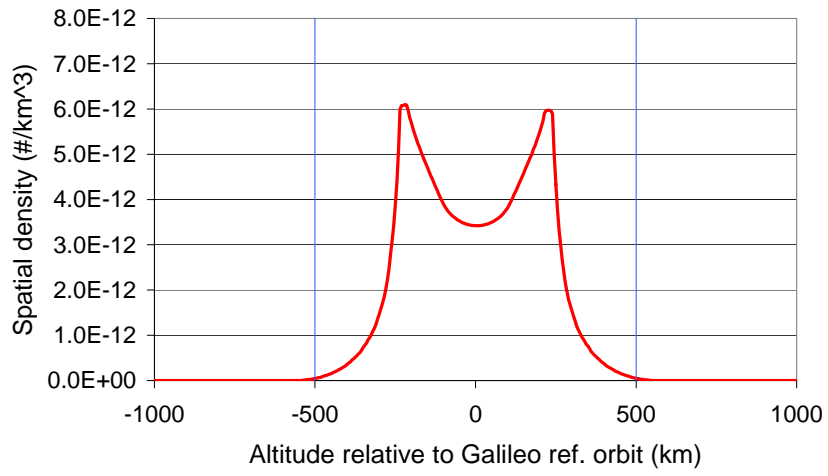


Figure 4. Variation of spatial number density with altitude (relative to the constellation reference orbit) of the Galileo constellation model used in this study. The spatial density is averaged over latitude.

6. Concept Of Collision Risk Dilution

In order to understand the concept of collision risk dilution, the dependence on orbital eccentricity of probability of collision posed by a sample disposed Galileo satellite was determined. The disposed satellite is assigned a semimajor axis $a = 30647$ km. When the eccentricity is 0.005, the perigee is 500 km above the Galileo reference circular orbit.

The collision probability posed by the disposed satellite to a secondary satellite on a circular orbit was computed as a function of the altitude of the secondary satellite. The collision probability is formulated from the perspective of the secondary satellite as it flies through the spatial density field of the disposed satellite. The formulation for computing the collision probability per unit time is then derived by simplifying Eq. 1 for the case when there is no time variation of the secondary satellite orbit.

$$\frac{dp_c}{dt}(h) = A_{cc} \rho_d(h) v(h) \quad (5)$$

where h is the altitude of the secondary satellite, $\rho_d(h)$ is the spatial density (averaged over latitude) of the disposed satellite at altitude h , $v(h)$ is the average relative velocity between the disposed and secondary satellites, and A_{cc} is the average collision cross-sectional area between the disposed vehicle and secondary satellites. As for the constellation, the spatial density $\rho_d(h)$ was computed using the formulation of Dennis/Kessler. The value of A_{cc} is set to unity, so the collision probability is normalized by collision cross-sectional area. The resulting formulation of collision probability assumes that the Ω and ω for the orbits are randomly and uniformly distributed over 360 deg.

Figure 5 shows the collision probability as a function of secondary satellite altitude. The eccentricity of the disposed satellite is varied parametrically. The plot shows that, as eccentricity increases, collision probability is significantly reduced for most altitudes between the apogee and perigee of the disposed satellite. The collision probability for an eccentricity of 0.36 is two orders of magnitude below the collision probability for an eccentricity of 0.005 for most altitudes. The reduction in collision probability at the altitude extremes is less substantial, especially at perigee. This indicates that, for a disposal orbit undergoing eccentricity growth, it is desirable to minimize the time spent by the disposal orbit perigee and apogee at altitudes with high population density.

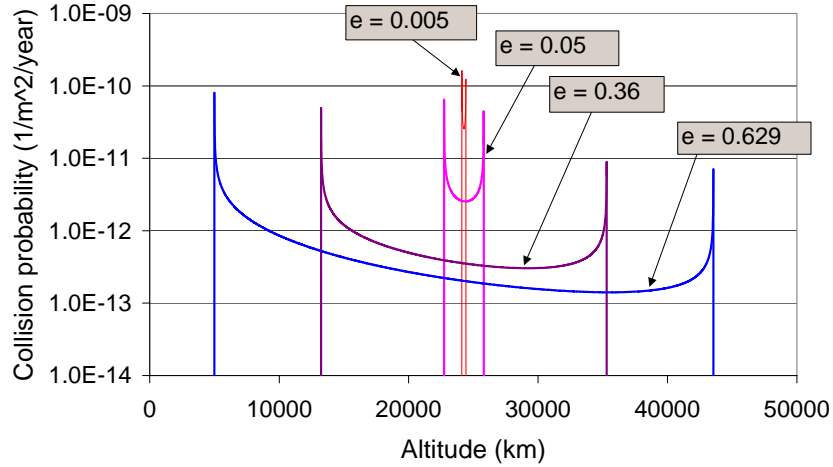


Figure 5. Collision risk posed by a disposed Galileo satellite to a target satellite on a circular orbit as a function of target satellite altitude.

It is also of interest to determine the collision risk between two disposed satellites with the same semimajor axis, eccentricity and inclination, but with different and randomly oriented Ω and ω . For this case, the collision probability was formulated from the perspective of one disposed satellite as it flies through the spatial density field of the other disposed satellite. The formulation of Eqs. 1-3 was used. (Eq. 4 was not needed because the in-plane orbital elements of the secondary satellite are static in this scenario.) As is done throughout the study, the value of A_{cc} is set to unity.

Figure 6 shows the resulting collision probability as a function of eccentricity. The plot shows that, as eccentricity increases, collision probability between the disposed satellites is significantly reduced. The collision probability for an eccentricity of 0.36 is one and a half orders of magnitude below the collision probability for an eccentricity of 0.005 for most altitudes.

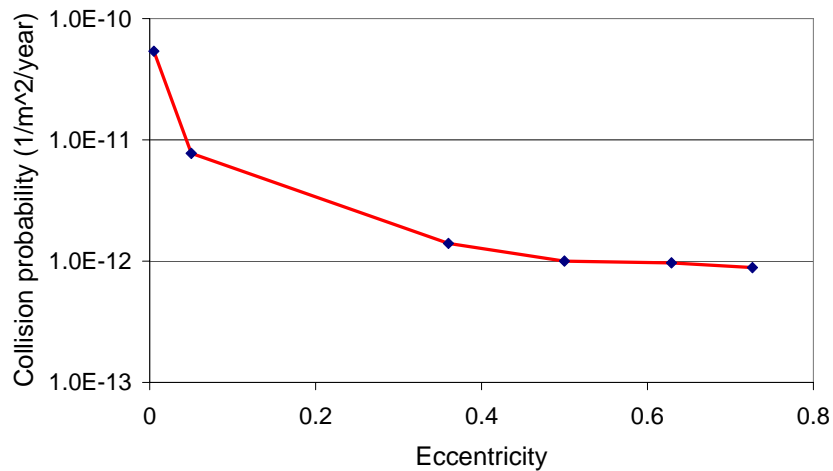


Figure 6. Collision risk between two disposed satellites as a function of eccentricity. Both satellites have the same semimajor axis, eccentricity and inclination but random Ω and ω .

7. Disposal Orbit Evolution For $E_0 = 0.005$

The long-term evolution was determined for a disposal orbit strategy with $e_0 = 0.005$ and perigee 500 km above the Galileo reference orbit. The corresponding semimajor axis is 30647 km. Initial inclination was assumed to be 56 deg. The first disposal is assumed to occur on 1 January 2009. As in the case for the constellation propagation, Ω_0 and ω_0 were varied over the range $[0, 360)$ deg in 10 deg increments. Orbital mean element vs. time profiles for each (Ω_0, ω_0) pair were generated by propagating over a time period of 200 years using MEANPROP.

Figures 7-8 show the resulting evolution of apogee and perigee altitude for a sample set of constellation orbits with $\Omega_0 = 0$ deg. Each pair of apogee and perigee curves corresponds to a specific value of ω_0 . From this plot it can be seen that values of ω_0 are available that result in either large, moderate, or small eccentricity growth. For some of the large eccentricity growth cases, the perigee drops low enough so that the disposed vehicle reenters the atmosphere toward the end of the 200-year time period. In addition, for some of the large eccentricity growth cases, the apogee altitude reaches and exceeds the altitude of geosynchronous orbit. However, a collision risk is only posed to geosynchronous satellites for relatively brief periods of time when the argument of perigee lies within one of four very narrow bands that depend on the current eccentricity of the disposal orbit.

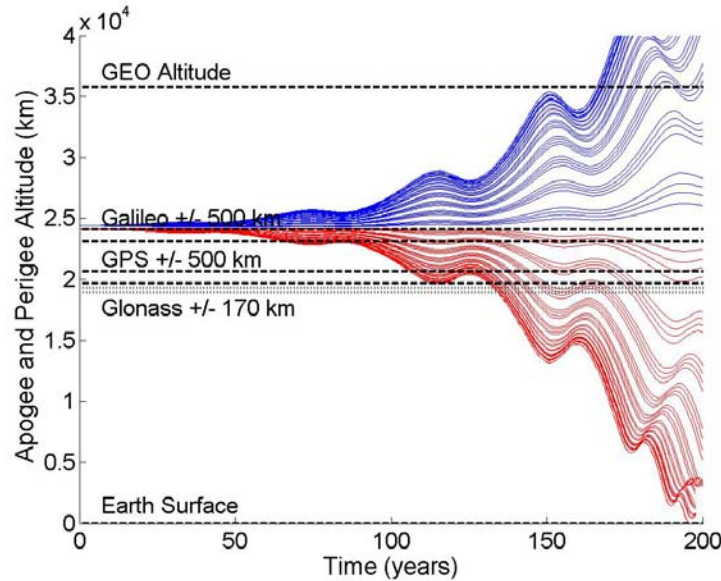


Figure 7. Apogee and perigee altitude profiles (shown relative to the Earth surface) of Galileo disposal orbits with $e_0 = 0.005$ for $\Omega_0 = 0$ deg. Curves are shown for values of ω_0 that span the range $[0, 360)$ deg in 10 deg increments.

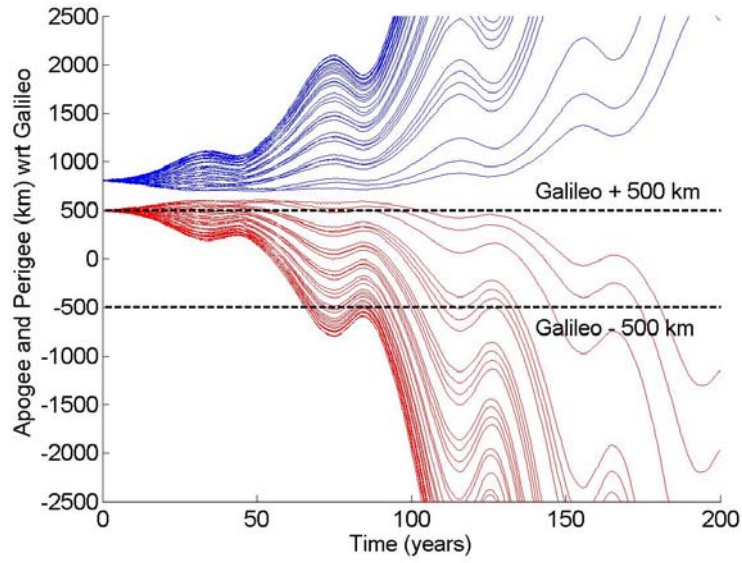


Figure 8. Apogee and perigee altitude profiles (shown relative to the constellation reference orbit) of Galileo disposal orbits with $e_0 = 0.005$ for $\Omega_0 = 0$ deg. Curves are shown for values of ω_0 that span the range $[0, 360)$ deg in 10 deg increments.

Figures 9-10 show the resulting evolution of apogee and perigee altitude for a sample set of constellation orbits with $\Omega_0 = 120$ deg. From this plot it can be seen that values of ω_0 are available that result in either moderate or small eccentricity growth, but not as large as for the case with $\Omega_0 = 0$ deg. There is no case where perigee drops low enough so that the disposed vehicle reenters within 200 years. There is also no case where apogee reaches GEO within 200 years.

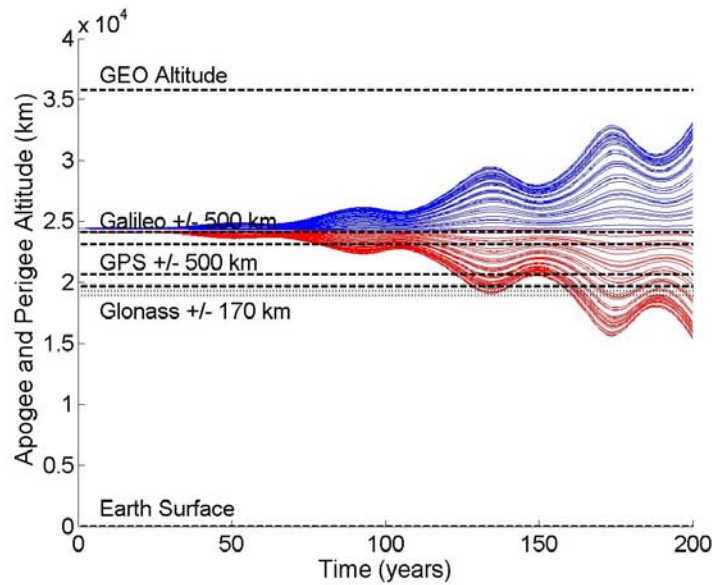


Figure 9. Apogee and perigee altitude profiles (shown relative to the Earth surface) of Galileo disposal orbits with $e_0 = 0.005$ for $\Omega_0 = 120$ deg. Curves are shown for values of ω_0 that span the range $[0, 360)$ deg in 10 deg increments.

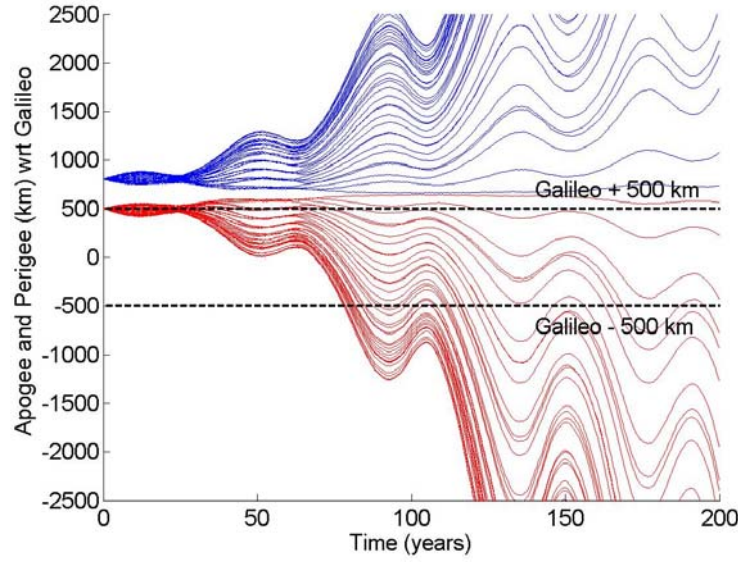


Figure 10. Apogee and perigee altitude profiles (shown relative to the constellation reference orbit) of Galileo disposal orbits with $e_0 = 0.005$ for $\Omega_0 = 120$ deg. Curves are shown for values of ω_0 that span the range $[0, 360)$ deg in 10 deg increments.

Figures 11-12 show the resulting evolution of apogee and perigee altitude for a sample set of constellation orbits with $\Omega_0 = 170$ deg. From this plot it can be seen that values of ω_0 are available that result in very small eccentricity growth. It is not possible to achieve moderate or large eccentricity growth.

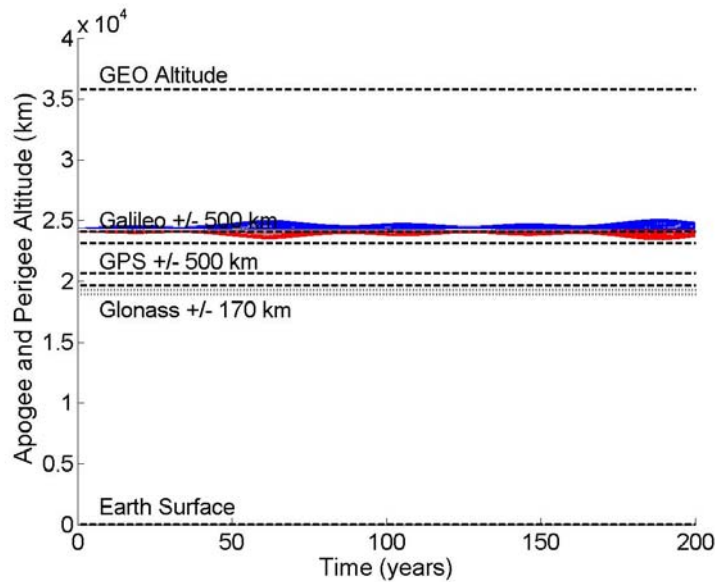


Figure 11. Apogee and perigee altitude profiles (shown relative to the Earth surface) of Galileo disposal orbits with $e_0 = 0.005$ for $\Omega_0 = 170$ deg. Curves are shown for values of ω_0 that span the range $[0, 360)$ deg in 10 deg increments.

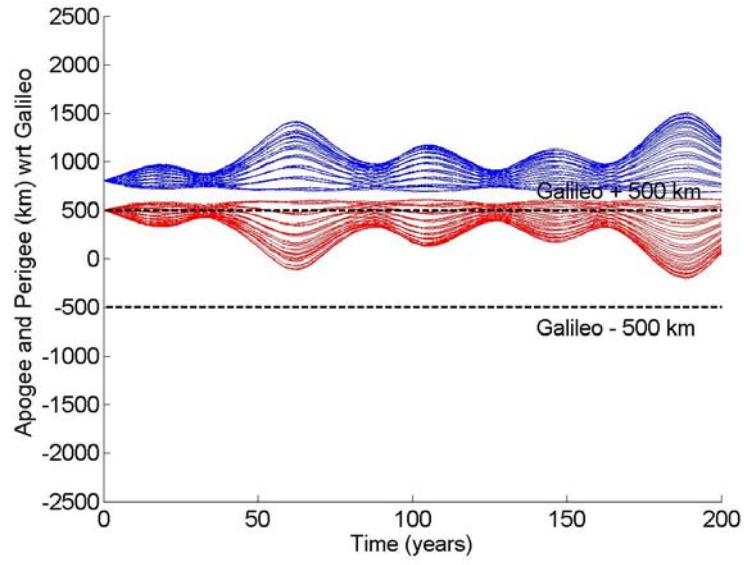


Figure 12. Apogee and perigee altitude profiles (shown relative to the constellation reference orbit) of Galileo disposal orbits with $e_0 = 0.005$ for $\Omega_0 = 170$ deg. Curves are shown for values of ω_0 that span the range $[0, 360)$ deg in 10 deg increments.

8. The Minimum Eccentricity Growth Strategy

Because of the strong sensitivity of eccentricity growth to ω_0 , a wide variety of disposal strategies are potentially available. The strategy that has been previously proposed is to minimize e_0 and select ω_0 that minimizes eccentricity growth. This strategy can be called the minimum eccentricity growth strategy. It will minimize the number of disposed vehicles that penetrate the constellation. By selecting the disposal orbit perigee to be 500 km above the constellation reference orbit, the ΔV required to clear the constellation is minimized.

There are several disadvantages with implementing this strategy. One disadvantage is that for small values of initial eccentricity, ω_0 becomes very sensitive to small maneuver errors, and it is difficult to accurately achieve a desired value of ω_0 .

Another disadvantage is that disposed vehicles will accumulate over time within a tightly confined graveyard. The disposed vehicles will experience in-track drift relative to each other due to initial orbit insertion errors and various orbital perturbations, such as solar radiation pressure. As a result the disposed satellites will pose a collision risk amongst themselves.

In order to model the graveyard population growth, a spatial density model of the graveyard was constructed as follows. At each value of Ω_0 over the range $[0, 360)$ deg, the value of ω_0 was selected that minimizes the eccentricity at the time point 100 years after disposal. The spatial density fields for each value of Ω_0 and each time point over the 200-year period were then computed and averaged together. The resulting averaged spatial density field represents one disposed satellite. To obtain the spatial density field that accounts for all satellites disposed up to a time t , the single satellite spatial density field was then multiplied by the number of accumulated disposed vehicles at time point t . This model represents a statistically stationary model of the graveyard in terms of its orbital dynamics, and is sufficiently accurate for the minimum eccentricity growth disposal strategy. It is not accurate for strategies that result in significant eccentricity growth, and is not used for such strategies in this study.

Figure 13 shows the spatial density field of the graveyard after 100 years, assuming a satellite disposal rate of 2 satellites per year. It is shown along with the spatial density field of the constellation. It is seen that the graveyard spatial density is much higher than the constellation spatial density.

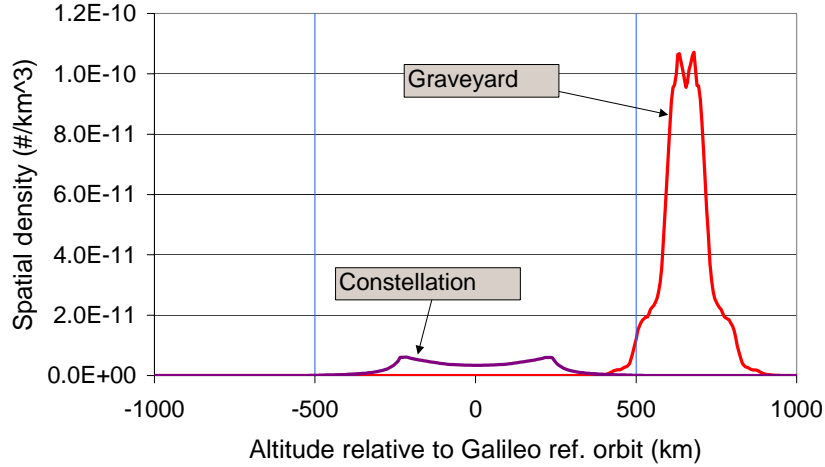


Figure 13. Spatial population densities of the graveyard and constellation after 100 years for the minimum eccentricity growth strategy.

The cumulative collision risk between the disposed vehicles in the graveyard was computed as a function of time. This was done as follows. The collision probability time profile was computed for a disposed satellite that flies through the spatial density field of a previously disposed satellite. The averaged single-satellite spatial density field that was determined for the graveyard was used to represent the previously disposed satellite. A collision probability profile was computed in this manner for each mean element vs. time profile in the ensemble that was used to generate the graveyard spatial density field.

The effect of a sequence of progressive satellite disposals was then modeled. For each subsequently disposed satellite, a collision probability vs. time profile was randomly selected from the ensemble of profiles (thereby modeling the random selection of Ω_0) and time-shifted to start at the time of the current disposal. Because that delayed collision probability time profile only accounts for the risk posed by one previously disposed vehicle, it is first multiplied by the number of previously disposed satellites and then added to the previously accumulated collision probability time profiles. This process is repeated until all vehicles disposed over the 200-year period have been included. The disposal sequence is then repeated 1000 times in Monte Carlo fashion.

This procedure yields an estimate of collision risk vs. time that is sufficiently accurate for this study because the eccentricity of the disposed satellites does not grow significantly. It accounts for the effect of the restricted dynamical variation of eccentricity over time on the graveyard spatial density.

Figure 14 shows the cumulative collision risk over time between disposed satellites in the graveyard. For comparison, the collision probability between the disposed satellites and the operational constellation is also shown. Both curves are the median profiles resulting from the Monte Carlo repetition of the disposal sequence. It is seen that, for most of the 200-year time period, the intra-graveyard collision risk is three to four orders of magnitude higher than the collision risk posed by the disposed vehicles to the constellation. As an example of the absolute collision risk, if the satellites have a collision cross-sectional area of 100 m^2 (corresponding to a collision radius of 5.64 m), the probability that a collision will occur sometime during the 200-year interval will be 0.02 (odds of one in 50).

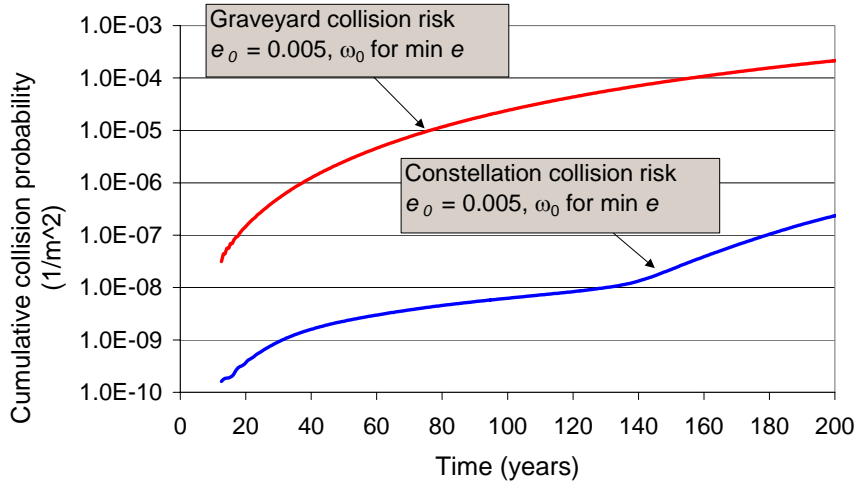


Figure 14. Cumulative collision risk over time between disposed satellites in the graveyard. For comparison, the collision probability between the disposed satellites and the operational constellation is also shown.

If a collision occurs between disposed vehicles in a graveyard that is located near the constellation, it is very likely that debris resulting from the collision will follow orbits that penetrate the constellation. This is due to the high relative velocities (typically on the order of 4.6 km/s) between disposed vehicles in combination with the relatively weak gravity field in MEO. Most of this debris will be smaller than the detection size threshold of tracking networks, and therefore it will not be possible for the constellation satellites to mitigate the risk they pose via collision prediction and avoidance. In contrast, the direct collision risk posed by intact disposed vehicles to the constellation can be mitigated via collision prediction and avoidance. Therefore, collision risk within the graveyard poses a significant indirect risk to the operational constellation.

One possible option to reduce the intra-graveyard collision risk is to require that subsequently disposed vehicles move to higher disposal orbits. The disadvantage of this strategy is that it will place a burden on the replacement satellites that will grow indefinitely over time.

9. High Eccentricity Growth Strategies

The option considered here is to exploit natural dilution of the intra-graveyard collision risk by increasing eccentricity growth. The strategy that is investigated here is to select (e_0 , ω_0) to maximize eccentricity growth at 100 years after disposal or, if atmospheric reentry can be achieved, to minimize time to reentry. The disposal orbit perigee is anchored at 500 km above the constellation reference orbit. An advantage of this strategy is that, as e_0 increases, it becomes easier to accurately target ω_0 . A disadvantage is that increasing e_0 must be accomplished by raising apogee. This will cost extra ΔV , so more effort on the part of the satellite will be required in the form of propellant as e_0 is increased. An important issue to consider is that the high eccentricity growth strategy will pose a higher direct collision risk to the constellation than the minimum eccentricity growth strategy. Therefore, the tradeoff between graveyard collision risk and constellation collision risk must be considered.

The high eccentricity growth strategy will also pose a higher direct collision risk to other objects external to Galileo, such as the GPS and Glonass systems and, in extreme cases, low Earth orbit and geosynchronous objects. Determination of the collision risk posed to these objects was beyond the scope of this study. However, it is expected to be low due to the dilutional effect of eccentricity growth as illustrated in Figs. 5-6. It is planned to quantify the comprehensive collision risk between all disposed, operational, and background objects in a future study.

Four levels of eccentricity were considered. Table 1 shows the corresponding disposal orbit semimajor axis and the required increase in semimajor axis above the constellation reference orbit for each level of eccentricity. For reference, $e_0 = 0.021$ will have an increase in semimajor axis of 1156 km. In comparison, the increase in semimajor axis for historical GPS disposals has ranged from 750 to 1350 km, with a range midpoint of 1050 km (Jenkin and Gick, 2003). Therefore, $e_0 = 0.021$ will have an effort that is roughly comparable to that of the mid-range of historical practice of GPS disposal. Eccentricities $e_0 = 0.036593$ and 0.051649 will require roughly 1.5 to 2 times the effort, respectively, of the mid-range of historical GPS practice. This range of disposal effort was selected for this study because it is believed to be feasible with modern satellite technology.

Table 1. High eccentricity growth strategy cases.

e_0	Perigee altitude rel. to Galileo (km)	Semimajor axis (km)	Increase in semimajor axis above Galileo (km)
0.005	500	30647	653
0.021051	500	31150	1156
0.036593	500	31652	1658
0.051649	500	32155	2161

The resulting apogee and perigee altitude profiles for $e_0 = 0.005$ have already been presented in Figs. 6-11. As noted before, large eccentricity growth, as well as re-entry within 200 years, can be achieved for some but not all values of Ω_0 .

Figures 15-17 show the apogee and perigee altitude profiles for $e_0 = 0.021$ and $\Omega_0 = 0, 120,$ and 170 deg respectively. It is seen that eccentricity growth has been increased, even for $\Omega_0 = 170$ deg. In addition, for $\Omega_0 = 0$, re-entry can be achieved within 140 years after disposal, and for $\Omega_0 = 120$, re-entry can be achieved within 200 years after disposal.

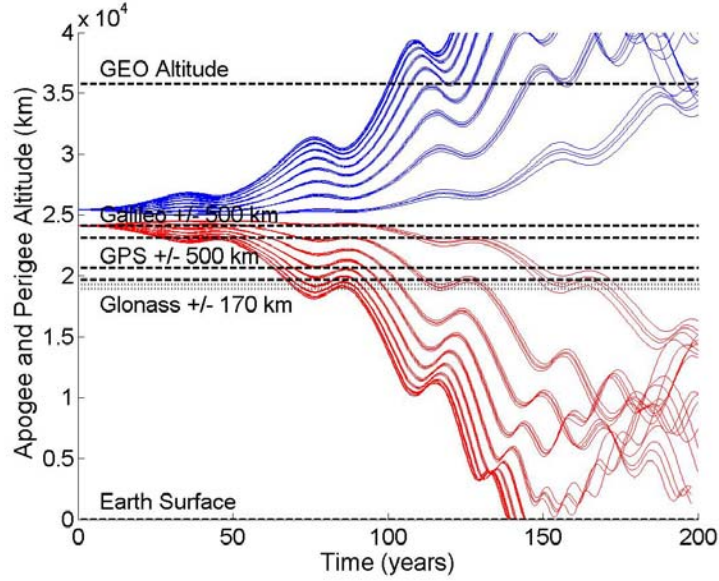


Figure 15. Apogee and perigee altitude profiles (shown relative to the Earth surface) of Galileo disposal orbits with $e_0 = 0.021$ for $\Omega_0 = 0$ deg. Curves are shown for values of ω_0 that span the range $[0, 360)$ deg in 10 deg increments.

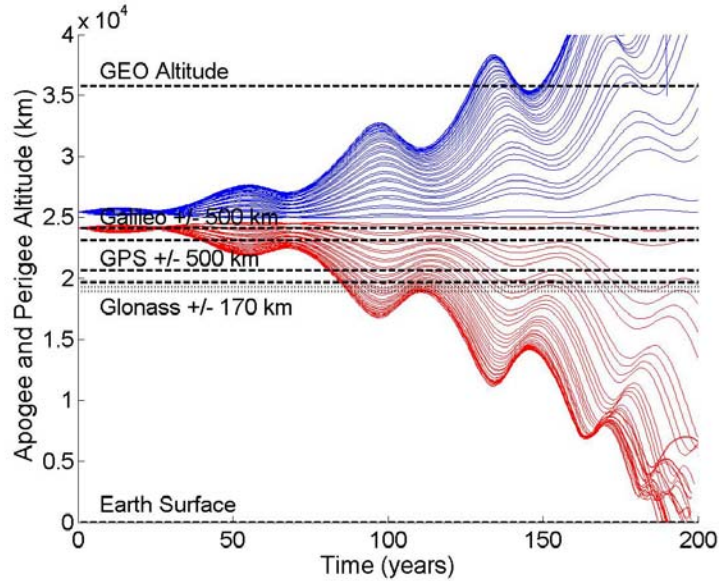


Figure 16. Apogee and perigee altitude profiles (shown relative to the Earth surface) of Galileo disposal orbits with $e_0 = 0.021$ for $\Omega_0 = 120$ deg. Curves are shown for values of ω_0 that span the range $[0, 360)$ deg in 10 deg increments.

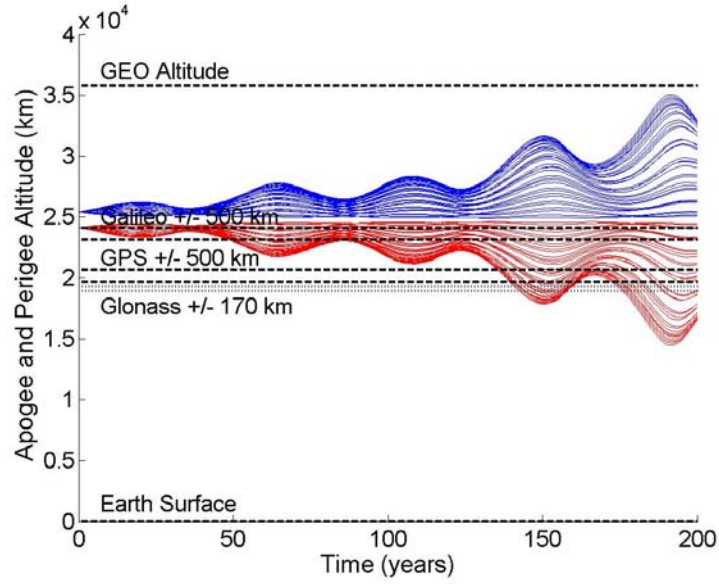


Figure 17. Apogee and perigee altitude profiles (shown relative to the Earth surface) of Galileo disposal orbits with $e_0 = 0.021$ for $\Omega_0 = 170$ deg. Curves are shown for values of ω_0 that span the range $[0, 360)$ deg in 10 deg increments.

Figures 18-20 show the apogee and perigee altitude profiles for $e_0 = 0.036593$ and $\Omega_0 = 290, 120$, and 170 deg respectively. It is seen that eccentricity growth has been increased further, especially for $\Omega_0 = 170$ deg. For $\Omega_0 = 120$ deg, re-entry can be achieved within 180 to 190 years after disposal. For $\Omega_0 = 290$ deg, re-entry can be achieved as early as 120 years after disposal.

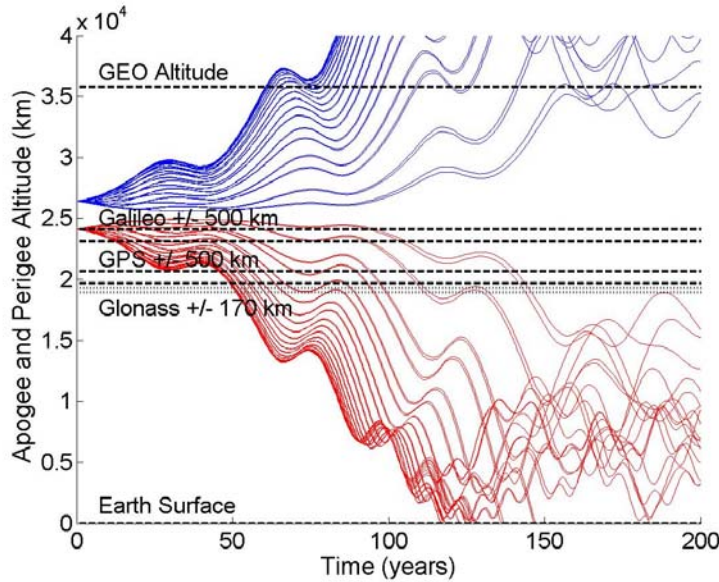


Figure 18. Apogee and perigee altitude profiles (shown relative to the Earth surface) of Galileo disposal orbits with $e_0 = 0.036593$ for $\Omega_0 = 290$ deg. Curves are shown for values of ω_0 that span the range $[0, 360)$ deg in 10 deg increments.

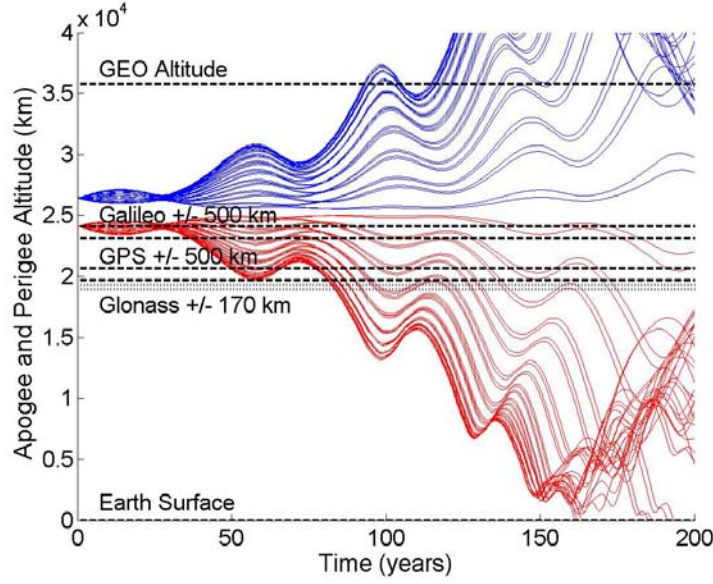


Figure 19. Apogee and perigee altitude profiles (shown relative to the Earth surface) of Galileo disposal orbits with $e_0 = 0.036593$ for $\Omega_0 = 120$ deg. Curves are shown for values of ω_0 that span the range $[0, 360)$ deg in 10 deg increments.

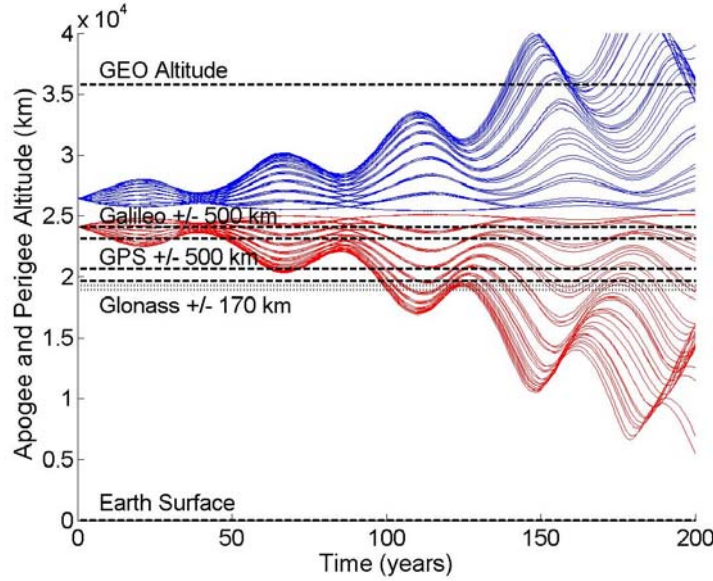


Figure 20. Apogee and perigee altitude profiles (shown relative to the Earth surface) of Galileo disposal orbits with $e_0 = 0.036593$ for $\Omega_0 = 170$ deg. Curves are shown for values of ω_0 that span the range $[0, 360)$ deg in 10 deg increments.

Figures 21-23 show the apogee and perigee altitude profiles for $e_0 = 0.051649$ and $\Omega_0 = 0, 120$, and 170 deg respectively. It is seen that, for $\Omega_0 = 0$ deg, the perigee altitude profiles undergo a reversal, and re-entry does not occur within 200 years. However, for $\Omega_0 = 120$ deg, re-entry can be achieved 130 years after disposal.

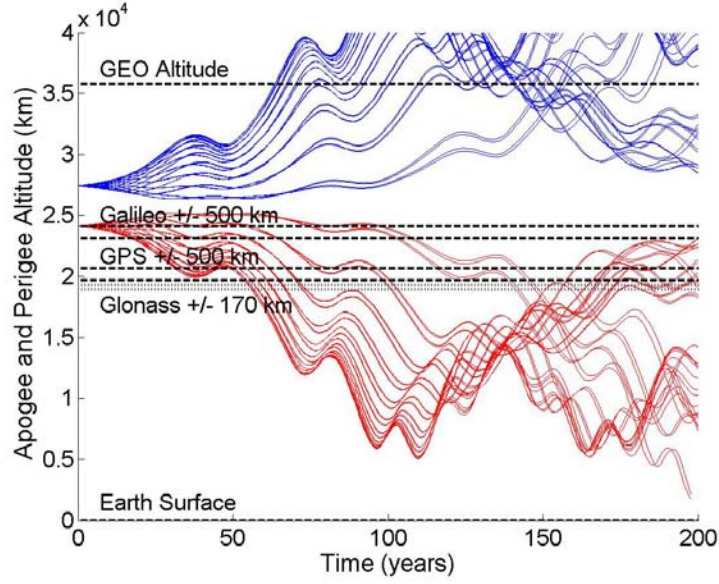


Figure 21. Apogee and perigee altitude profiles (shown relative to the Earth surface) of Galileo disposal orbits with $e_0 = 0.051649$ for $\Omega_0 = 0$ deg. Curves are shown for values of ω_0 that span the range $[0, 360)$ deg in 10 deg increments.

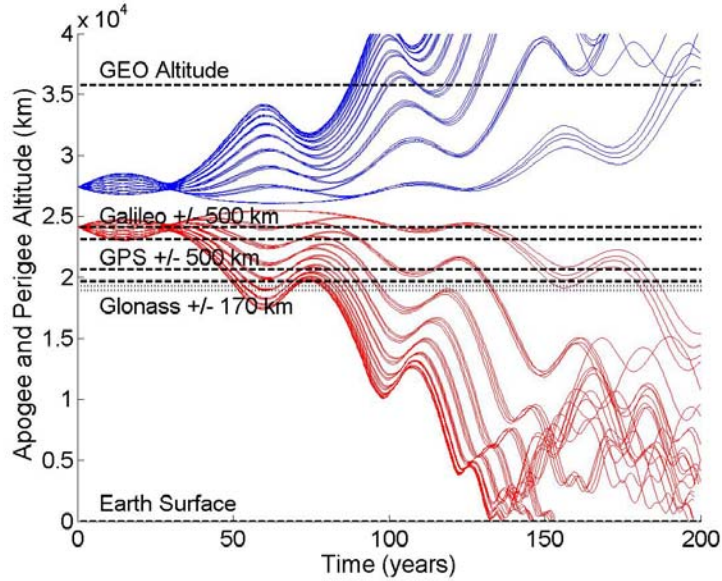


Figure 22. Apogee and perigee altitude profiles (shown relative to the Earth surface) of Galileo disposal orbits with $e_0 = 0.051649$ for $\Omega_0 = 120$ deg. Curves are shown for values of ω_0 that span the range $[0, 360)$ deg in 10 deg increments.

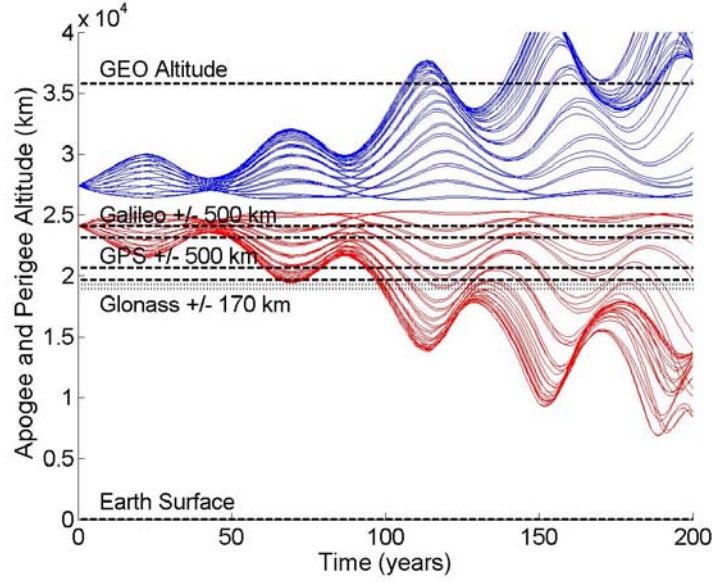


Figure 23. Apogee and perigee altitude profiles (shown relative to the Earth surface) of Galileo disposal orbits with $e_0 = 0.051649$ for $\Omega_0 = 170$ deg. Curves are shown for values of ω_0 that span the range $[0, 360)$ deg in 10 deg increments.

Figure 24 shows the time profiles of collision risk posed to the constellation by accumulating disposed vehicles (assuming a disposal rate of two per year) corresponding to the various disposal strategies. The plot shows curves for the four high eccentricity growth cases considered, and also a strategy in which $e_0 = 0.005$, perigee is 500 km above the constellation reference orbit, and ω_0 is not specifically targeted but rather allowed to vary randomly among sequentially disposed satellites. From the plot, it is seen that the case with the highest collision risk is the high eccentricity growth case with $e_0 = 0.005$. The case with the second highest collision risk after 130 years is the random ω_0 case with $e_0 = 0.005$. The long-term collision risk is reduced further for the high eccentricity growth strategy cases with higher e_0 . The collision risk is continually reduced as e_0 is increased, however the gains in risk reduction begin to diminish after e_0 exceeds 0.036593.

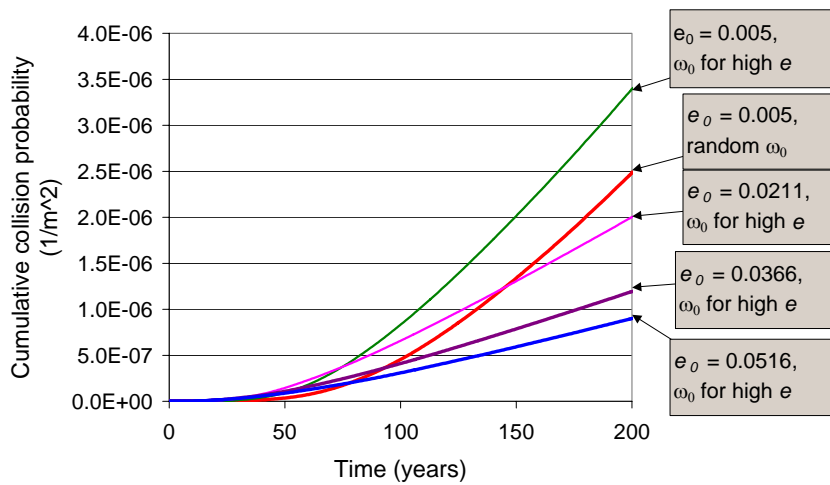


Figure 24. Collision risk posed to the Galileo constellation by various disposal strategies.

Figure 25 shows the collision risk posed to the constellation for the disposal strategies considered, including the minimum eccentricity growth case, along with the intra-graveyard collision risk for the minimum eccentricity growth case. It is necessary to use a logarithmic plot in order to show the broad range of collision risk that is encompassed. It is seen that the high eccentricity growth strategies and the random ω_0 strategy result in a higher collision risk to the constellation than the minimum eccentricity growth strategy. However, the collision risk posed to the constellation by the high eccentricity growth strategies is much lower than the intra-graveyard collision risk. The high eccentricity growth strategy with $e_0 = 0.036593$ produces a constellation risk that is more than two orders of magnitude below the graveyard risk for the minimum eccentricity growth strategy.

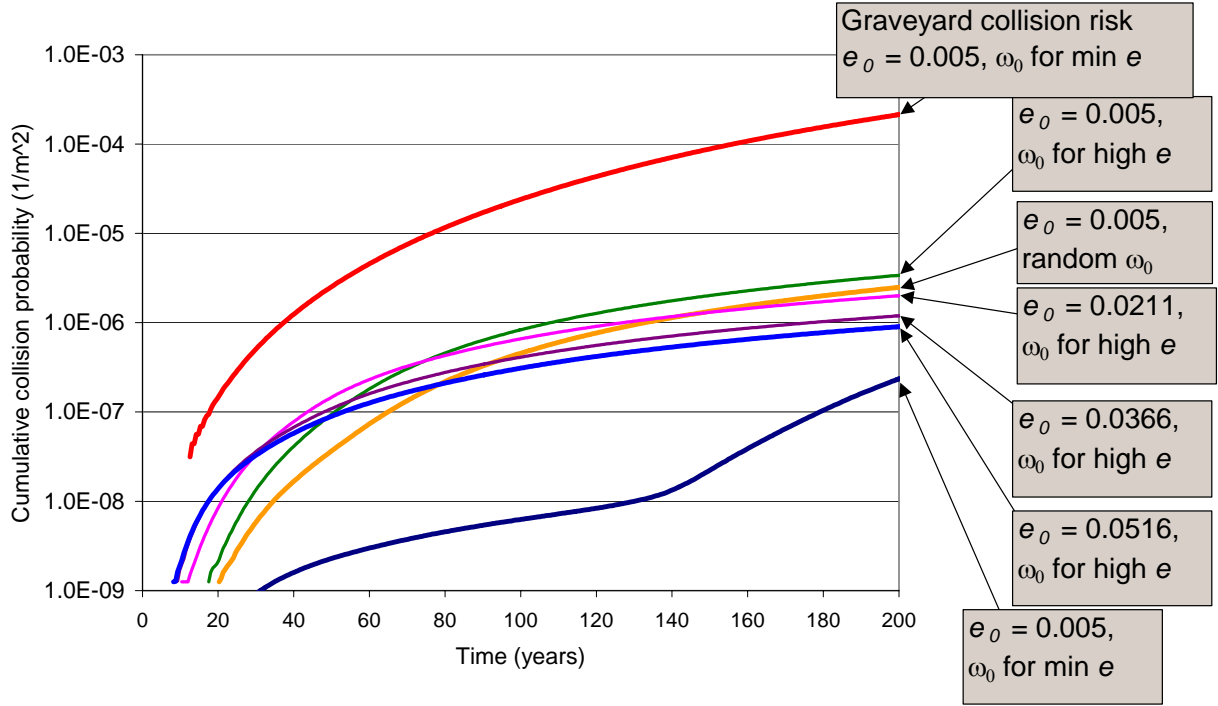


Figure 25. Comparison of the collision risk posed to the constellation by various disposal orbit strategies with the intra-graveyard collision risk for the minimum eccentricity growth strategy.

The intra-graveyard collision risk for the high eccentricity growth strategies was not quantified in this study. However, from Fig. 6 it is expected that these strategies will significantly reduce the intra-graveyard collision risk. Therefore, the combined constellation and graveyard collision risk associated with Galileo can be significantly reduced by using the high eccentricity growth strategy as long as e_0 is large enough.

Table 2 shows the percentage of disposed satellites that will re-enter within 200 years after disposal for various strategies. The results account for the entire $[0,360)$ deg range of Ω_0 . It is seen that the re-entry percentage is significantly increased and is substantial for the high eccentricity growth cases with $e_0 = 0.0211$ and larger.

Table 2. Percentage of satellites that re-enter within 200 years after disposal.

ω_0 -selection strategy	e_0	% of satellites that reenter before 200 years after disposal
Random ω_0	0.005	7.1%
High eccentricity	0.005	19%
"	0.0211	67%
"	0.036593	75%
"	0.051649	92%

10. Conclusions

The study presented here investigated the possibility of diluting MEO disposal orbit collision risk by selection of initial disposal orbit eccentricity and argument of perigee in order to control long-term eccentricity growth. The Galileo constellation was selected as an example.

Various disposal strategies were considered. The minimum eccentricity growth strategy minimizes the collision risk posed directly to the constellation by accumulating disposed vehicles. However, it also results in a risk of collision between disposed vehicles in the graveyard that is much higher than the risk posed directly to the constellation. The minimum eccentricity growth strategy also has the disadvantage that it is difficult to accurately target argument of perigee, thereby making it difficult to attain the desired eccentricity growth profile.

High eccentricity growth strategies increase the collision risk posed directly to the constellation, but they will significantly reduce the intra-graveyard collision risk. Therefore, the high eccentricity growth strategies will reduce the combined constellation and intra-graveyard collision risk. The increase in collision risk posed to the constellation can be reversed by increasing initial disposal orbit eccentricity. The high eccentricity growth strategies also have the advantage that it is easier to accurately target argument of perigee, thereby making it easier to attain the desired eccentricity growth profile.

It is preferable to avoid a high graveyard collision risk because potential graveyard collisions can produce untrackable debris that will penetrate the constellation and cannot be evaded by collision avoidance.

Determination of the collision risk posed to objects external to the Galileo system was beyond the scope of this study. However, it is expected to be low due to the dilutional effect of eccentricity growth. It is planned to quantify the comprehensive collision risk between all disposed, operational, and background objects in a future study.

High eccentricity growth strategies also offer the option of significantly increasing the percentage of disposed vehicles that will re-enter the atmosphere within 200 years after disposal rather than remain on orbit for thousands of years. This option may be desirable if the vehicles are designed to pose an acceptably low ground casualty expectation.

Therefore, both in terms of collision risk reduction and removal of disposed vehicles from orbit, the strategy of achieving high eccentricity growth by selection of initial disposal orbit eccentricity and argument of perigee offers an effective and potentially inexpensive option for MEO debris mitigation.

References

- Chao, C.C., "MEO Disposal Orbit Stability and Direct Reentry Strategy," *Advances in the Astronautical Sciences*, Vol. 105, January 2000, pp. 817-838.
- Chao, C.C., and Gick, R.A., "Long-Term Evolution of Navigation Satellite Orbits: GPS/GLONASS/GALILEO," *Advances in Space Research*, Vol. 34, Issue 5, 2004, pp 1221-1226.
- Dennis, N.G., "Probabilistic Theory and Statistical Distribution of Earth Satellites," *Journal of the British Interplanetary Society*, Vol. 25, 1972, pp. 333-376.
- ESA, "Galileo: Mission High Level Definition," http://europa.eu.int/comm/dgs/energy_transport/galileo/doc/galileo_hld_v3_23_09_02.pdf, September 23, 2002.
- Gick, R.A., and Chao, C.C., "GPS Disposal Orbit Stability and Sensitivity Study," *Advances in the Astronautical Sciences*, Vol. 108, February 2001, pp. 2005-2018.
- Jenkin, A.B., and Gick, R.A., "Collision Risk Associated with Instability of MEO Disposal Orbits," Sawaya-Lacoste, H., editor, *Proceedings of the Third European Conference on Space Debris*, ESA SP-473, Vol. 1, Darmstadt, Germany, October 2001, pp. 471-476.
- Jenkin, A.B., and Gick, R.A., "Collision Risk Posed to the Global Positioning System by Disposal Orbit Instability," *Journal of Spacecraft and Rockets*, Vol. 39, No. 4, July-August 2002.
- Jenkin, A.B., and Gick, R.A., "Collision Risk Posed to the Global Positioning System by Disposed Upper Stages," IAC-03-IAA.5.3.01, International Astronautical Congress 2003, Bremen, Germany, October 2, 2003.
- Kessler, D.J., "Derivation of the Collision Probability between Orbiting Objects: The Lifetimes of Jupiter's Outer Moons," *Icarus* 48, 1981, pp. 39-48.
- McClain, W.D., "A Recursively Formulated First-Order Semianalytic Artificial Satellite Theory Based on the Generalized Method of Averaging," Computer Sciences Corporation, CSC/TR-77/6010, Greenbelt, MD, November 1977.
- Space Daily, "ESA Checks Over First Galileo Experimental Satellite Model," September 24, 2004.